Magnetic Materials

DOI: 10.1002/anie.200801482

A Perovskite Containing Quadrivalent Iron as a Charge-Disproportionated Ferrimagnet**

Ikuya Yamada, Kazuhide Takata, Naoaki Hayashi, Satoshi Shinohara, Masaki Azuma, Shigeo Mori, Shigetoshi Muranaka, Yuichi Shimakawa, and Mikio Takano*

A large number of oxides containing Fe^{II} and/or Fe^{III} are known, whereas only a few, like $(Sr,Ca)Fe^{IV}O_3$[1–3] and $K_2Fe^{VI}O_4$, contain iron in higher oxidation states.[4] During the course of our exploration of *A*-site-ordered perovskites with the general formula $AA'_3B_4O_{12}$, we successfully obtained $CaCu^{II}_3Fe^{IV}_4O_{12}$ (CCFO), which is the first Fe^{IV} oxide to be discovered in almost three decades. CCFO has been found to undergo an interesting phase transition to a charge-disproportionated ferrimagnetic state at 210 K. This charge disproportionation (CD) is of the $CaFeO_3$ (CFO) type ($2Fe^{IV} \rightarrow Fe^{III} + Fe^{V}$)[5] and is accompanied by a structural transition that leaves these aliovalent species ordered in the rock-salt manner.[6,7] The magnetic behavior of these two species is strikingly different however: CCFO features a large spontaneous magnetization whereas CFO is an antiferromagnet with a relatively low Néel temperature of 116 K.[3]

CCFO forms in a solid-state reaction at pressures above 9 GPa and a temperature of around 1300 K. However, we noticed during the characterization process that Fe^{III} tends to substitute at the *A'* site and that the amount decreases as the applied pressure increases. The amount of impurities also decreased in the same manner. The sample to be discussed here was prepared at the highest available pressure of 15 GPa. Synchrotron X-ray powder diffraction (SXRD) at room temperature followed by a Rietveld refinement confirmed the desired Ca/Cu-ordering in a cubic perovskite cell of $2a_0 \times 2a_0 \times 2a_0$ (a_0: simple perovskite cube; Figure 1a and Table 1).

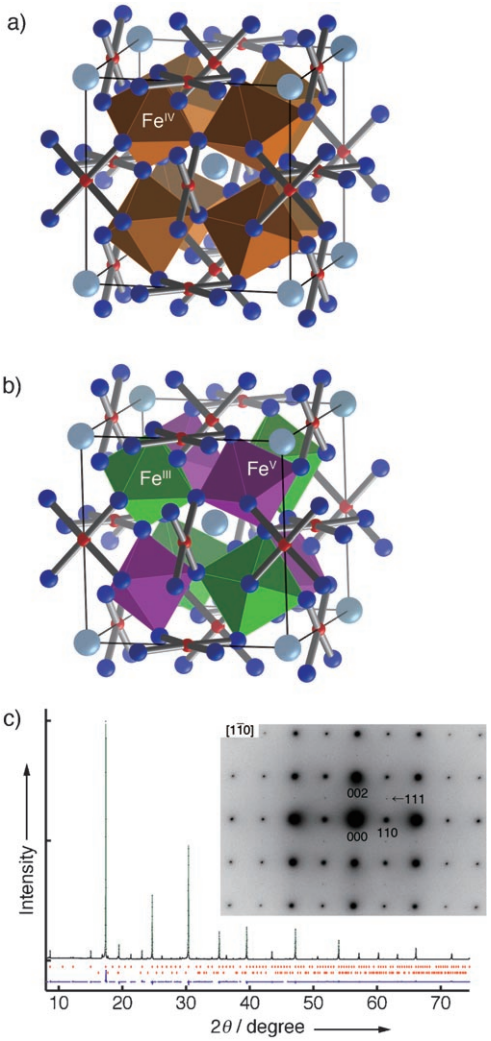

Figure 1. Crystal structures a) before and b) after the charge disproportionation. Ca gray, O blue, Cu red. c) SXRD pattern measured at 90 K and the result of the Rietveld refinement. The dots and the solid line represent the observed data and fitted pattern, respectively. The vertical marks show the Bragg peaks of CCFO (upper) and CuO (bottom). The bottom curve represents the difference between the observed and calculated patterns. The inset shows an ED pattern for the [$\bar{1}$10] incidence taken at 120 K.

[*] Dr. I. Yamada,[+] K. Takata, Prof. M. Azuma, Prof. Y. Shimakawa, Prof. M. Takano[#]
Institute for Chemical Research
Kyoto University
Gokasho, Uji, Kyoto 611-0011 (Japan)
Fax: (+81) 774-38-3118

Prof. N. Hayashi, Prof. S. Muranaka
Graduate School of Human and Environmental Studies
Kyoto University, Kyoto 606-8501 (Japan)

S. Shinohara, Prof. S. Mori
Department of Physics
Osaka Prefecture University, Osaka 599-8531 (Japan)

[+] Present address: Graduate School of Science and Engineering
Ehime University
2–5, Bunkyo-Cho, Matsuyama, Ehime 790-8577 (Japan)
Fax: (+81) 89-927-9590
E-mail: ikuya@chem.sci.ehime-u.ac.jp

[#] Present address: Institute for Integrated Cell-Material Sciences
Kyoto University
c/o Research Institute for Production Development
Kyoto 606-0805 (Japan)

[**] This work was partly supported by Grants-in-Aid for Scientific Research (grant nos. 19GS0207, 18350097, 17105002, 19014010, 19340098, 19052008) and by the MEXT Joint Project of Chemical Synthesis Core Research Institutions. I.Y. was financially supported by 21COE on the Kyoto Alliance for Chemistry The synchrotron radiation experiments were performed at the SPring-8 with the approval of the Japan Synchrotron Radiation Research Institute.

Supporting information for this article is available on the WWW under http://dx.doi.org/10.1002/anie.200801482.

Table 1: Structure parameters refined from SXRD data collected at room temperature and 90 K.

Atom	Site	*g*	*x*	*y*	*z*	1000 *U* [Å^2]
			Room temperature			
Ca	2*a*	1[a]	0	0	0	10.9(4)
Cu	6*b*	0.968(12)[b]	0	0.5	0.5	6.27(16)[b]
Fe1	6*b*	0.032(12)[b]	0	0.5	0.5	6.27(16)[b]
Fe2	8*c*	1[a]	0.25	0.25	0.25	0.67(12)
O	24*g*	1[a]	0.30809(13)	0.17818(15)	0	7.6(2)
			90 K			
Ca	2*a*	1[a]	0.5	0.5	0.5	11.5(5)
Cu	6*d*	0.968[c]	0.5	0	0	5.60(14)[d]
Fe1	6*d*	0.032[c]	0. 5	0	0	5.60(14)[d]
Fe2	4*b*	1[a]	0.25	0.25	0.25	1.60(12)[e]
Fe3	4*c*	1[a]	0.75	0.75	0.75	1.60(12)[e]
O	24*h*	1[a]	0.5056(5)	0.67955(16)	0.80732(14)	9.1(3)

The space group is $Im\bar{3}$ (no. 204) and $Pn\bar{3}$ (no. 201) at room temperature and 90 K, respectively. The lattice constant *a* is 7.29546(3) and 7.26122(4) Å at room temperature and 90 K, respectively. The goodness of fit (*S*) and the *R* factors are $S=1.55$, $R_{wp}=2.79\,\%$, and $R_I=2.41\,\%$ at room temperature and $S=1.84$, $R_{wp}=2.96\,\%$, and $R_I=4.34\,\%$ at 90 K. [a] Site occupancies *g* for Ca, Fe2, Fe3, and O were fixed to be unity. [b] The following constraints were used for the 6*b* site: $g(\mathrm{Cu})+g(\mathrm{Fe1})=1$, $U(\mathrm{Cu})=U(\mathrm{Fe1})$. [c] Occupancies at the 6*d* site were fixed to the values refined at room temperature. [d] The following constraint was used for the 6*d* site: $U(\mathrm{Cu})=U(\mathrm{Fe1})$. [e] The following constraint was used for the 4*b* and 4*c* sites: $U(\mathrm{Fe2})=U(\mathrm{Fe3})$.

However, small amounts of CuO (ca. 1.8 wt %) and unidentified phases were still observed in the SXRD data. The amount of Fe^{III} ions at the *A*′ site ($Fe^{III}A'$) was estimated from the structural analysis to be 3 atom %, which is consistent with the Mössbauer spectroscopic estimation of about 4 atom %. There was no indication of Cu^{II} or Cu^{III} substitution at the *B* site. The bond valence sums[8] (BVS) for Cu and Fe (+2.43 and +3.77, respectively) are rather unusual and suggest a considerable charge transfer between the CuO_4 and FeO_6 units.[9]

The resistivity of a sintered pellet of CCFO (approx. $2\times10^{-2}\,\Omega\,\mathrm{cm}$) is essentially temperature-independent above 210 K, although it increases quickly below this temperature (Figure 2). This temperature increases slightly under increasing magnetic field, thus suggesting a phase transition to a more resistive and magnetic phase. Indeed, a spontaneous magnetization was observed (Figure 3 a).It is interesting to compare two simple magnetic models, one of which is ferromagnetic, Cu^{II}-$(S=1/2,\uparrow)_3Fe^{IV}(S=2,\uparrow)_4$ and the other is ferrimagnetic, $Cu(\downarrow)_3Fe(\uparrow)_4$. The experimental saturation magnetization of (M_s) of 9.7 μ_B per formula unit estimated as in Figure 3 b is closer to the ferrimagnetic moment of 13 μ_B per formula unit rather than the ferromagnetic moment of 19 μ_B per formula unit. Essentially the same ferrimagnetic spin structure is known for $CaCu_3Mn_4O_{12}$.[10] Experimentally, the magnetization was found to decrease as the amount of $Fe^{III}A'$ increased, although the transition temperature, T_C, did not change significantly. It therefore appears that $Fe^{III}A'$ disturbs the magnetism strongly but only in a limited region. Both the resistivity and the magnetization tend to level off or even decrease at around 70 K, although the reason for this is not yet clear.

Microscopic details were studied by Mössbauer spectroscopy. The spectrum taken at room temperature (Figure 4) consists of three superimposed components in a 93:4:3 ratio, these are: *i*) a singlet with an isomer shift (IS) of 0.15 $\mathrm{mm\,s^{-1}}$ relative to α-Fe, *ii*) a quadrupole doublet with IS = 0.38 $\mathrm{mm\,s^{-1}}$ and a quadrupole splitting

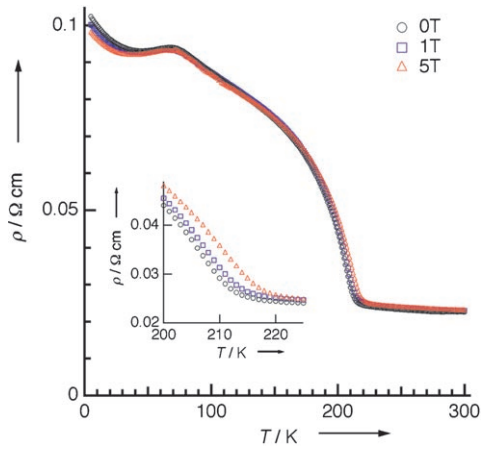

Figure 2. Temperature dependence of the electrical resistivity of a sintered pellet between 5 and 300 K. The inset shows an enlargement of the region around the transition temperature.

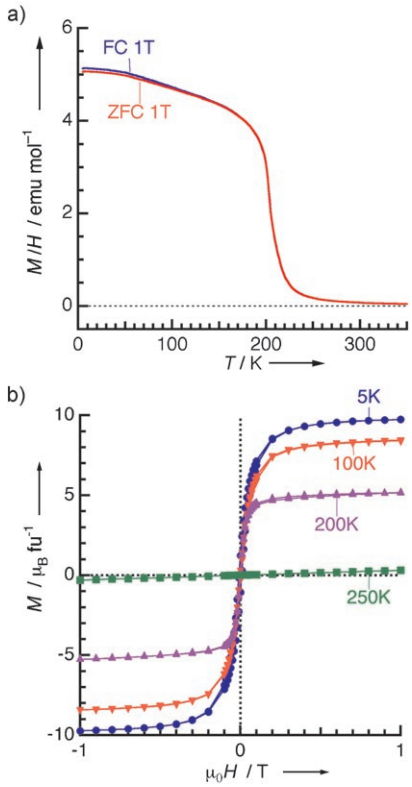

Figure 3. a) Temperature dependence of the dc magnetization divided by field (M/H) measured in an external magnetic field of 1 T on field cooling (FC) and on heating after zero-field cooling (ZFC) between 5 and 300 K. b) M–H curves measured at various temperatures.

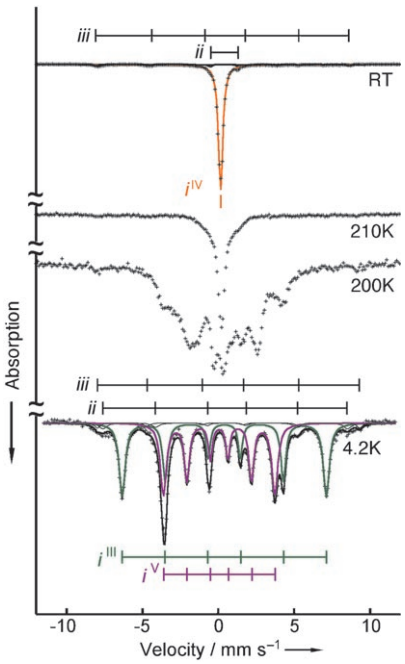

Figure 4. Mössbauer spectra taken at various temperatures. The dots and the solid lines represent the observed spectra and the fittings, respectively. The components at 4.2 K are: i^{IV}: Fe^{IV} occupying the *B*-site; *ii*: Fe^{III} substituting for Cu^{II} at the *A′* site; *iii*: α-Fe_2O_3 impurity; i^{III}: Fe^{III} at the *B* site; i^{V}: Fe^{V} at the *B* site.

(ΔE) of 1.83 mm s^{-1}, and *iii*) a magnetic sextuplet, which is due to an α-Fe_2O_3 impurity. We note here that this impurity was not detected in the SXRD measurement, probably because it was removed during the sedimentation step in the sampling process. The IS of the first of these components, which is the major Fe^{IV} species at the *B* site ($Fe^{IV}B$), is considerably larger than those (approx. 0.07 mm s^{-1}) reported previously for CFO and $SrFeO_3$,[1,5,11] thus indicating that its real electronic state is slightly closer to Fe^{III}. This interpretation is consistent with the charge transfer suggested from the BVS calculation mentioned above. The second component, which has an Fe^{III}-like IS, was assigned to $Fe^{III}A'$. The large quadrupole splitting of this component most likely reflects the strong anisotropy of the square coordination, and its amount is consistent with the SXRD result. A similar $Fe^{III}A'$ species has also been observed for a related oxide of $CaMn_7O_{12}$ doped with ^{57}Fe for use as a Mössbauer spectroscopic probe and $CaCu_3Mn_{4-x}Fe_xO_{12}$.[12,13]

The spectra below T_C are magnetically split. Furthermore, as can be seen clearly in the spectrum recorded at 4.2 K, the $Fe^{IV}B$ component is divided into two subcomponents (i^{III} and i^{V}) with very different hyperfine parameters but equal intensities, thereby revealing the occurrence of a CD of the CFO type. The IS values for Fe^{III} (i^{III}) and Fe^{V} (i^{V}) at 4.2 K are 0.39 and 0.05 mm s^{-1}, respectively, and their magnetic hyperfine fields are 41.7 and 22.7 T, respectively. It is not yet clear whether the transition at 210 K is first or second order in nature, although it is clear that the magnetic ordering, the CD, and the resistivity change occur concomitantly.

Structural studies on the low-temperature (LT) phase using electron diffraction (ED) and SXRD revealed a rock-salt type ordering of Fe^{III} and Fe^{V}, as can be seen from the appearance of the (111) reflection in the inset to Figure 1c. The lattice symmetry is lowered to $Pn\bar{3}$ and there is a sudden decrease in the lattice constant (see the Supporting Information). The LT structure contains two kinds of *B*-sites (4*b* and 4*c*) arranged in the rock-salt manner, see Figure 1b. According to the SXRD analysis at 90 K, the Fe–O bonds are 1.970(3) and 1.893(3) Å for Fe^{III} ($Fe^{III}B$) and Fe^{V} ($Fe^{V}B$), respectively, as is also in the case for CFO[6,7] (see the Supporting Information). The BVSs of 3.51 and 4.33 for these ions at 90 K also confirm the CD. In light of the above, the aforementioned spin structure of $Cu^{II}(S=1/2,\downarrow)_3Fe^{IV}(S=2,\uparrow)_4$ should therefore be written as $Cu^{II}(S=1/2,\downarrow)_3Fe^{III}(S=5/2,\uparrow)_2Fe^{V}(S=3/2,\uparrow)_2$, although there is no difference in the magnitude of the resulting magnetization between these.

The magnetism of the LT phase seems to be very different from the antiferromagnetism of CFO. However, if we recall that a pair of nearest neighboring Fe atoms orient their moments away from each other in the helicoidal spin structure of CFO by only around 45°,[14,15] these oxides could be considered to be rather similar to each other. The presence of Cu at an *A′*-site ($Cu^{II}A'$) must produce a perturbation that leads to the repression of the original spin canting. This perturbation arises from the aforementioned inter-site charge transfer, antiferromagnetic *A′*–*B* interactions, and a change in the Fe–O–Fe bond lengths and bond angles. We have assigned the lower value of the experimental saturation magnetization compared with the calculated ferrimagnetic moment to strong, but localized, disturbances caused by $Fe^{III}A'$. The electronic interactions through the $Fe^{III}A'(S=5/2)$–O–Fe^{III}/$Fe^{V}B$ coupling should be drastically different from those through $Cu^{II}A'(S=1/2)$-O-Fe^{III}/$Fe^{V}B$ and the lattice must be more or less distorted locally. The resulting magnetic disturbances seem to be quite remarkable experimentally.

In summary, we have succeeded in synthesizing a new Fe^{IV}-perovskite ($CaCu_3Fe_4O_{12}$) by means of high-pressure synthesis. This oxide shows a CFO-type charge disproportionation ($2Fe^{IV} \rightarrow Fe^{III} + Fe^{V}$) at $T_C = 210$ K, which is accompanied by an electrical, magnetic, and structural change. The magnetic structure is most probably $Cu^{II}(S=1/2,\downarrow)_3Fe^{III}(S=5/2,\uparrow)_2Fe^{V}(S=3/2,\uparrow)_2$. It is known that Fe^{IV} has very low-lying 3d levels and that the resulting covalent electronic state can be expressed as $Fe^{III}\underline{L}$, where $\underline{L}$ represents a ligand hole.[16] In the present oxide, $Cu^{II}\underline{L}A'$ competes with $Fe^{IV}B$ for the ligand holes and the antiparallel *A′*–*B* spin arrangement in the LT phase suppresses the conduction of holes.

Experimental Section

$CaCO_3$ (Rare metallic, 99.99%), CuO (Rare metallic, 99.99%), α-Fe_2O_3 (Rare metallic, 99.99%) and $KClO_4$ (Wako, 99%) were used.

$Ca_2Fe_2O_5$ was synthesized from a mixture of $CaCO_3$ and Fe_2O_3 in advance, then a 1:6:3 molar mixture of $Ca_2Fe_2O_5$, CuO, and Fe_2O_3 and $KClO_4$ (23 wt%) as oxidizing agent were charged into a gold capsule and heated at 1300 K and 15 GPa for 30 min in a Kawai-type high-pressure apparatus. The powder samples for XRD, magnetic susceptibility, and Mössbauer spectroscopy measurements were prepared by washing the synthetic products with distilled water, ethanol, and acetone in turn. The sample for electrical resistivity measurement was

obtained by sintering the powder at 8 GPa and 1000 °C with $KClO_4$ in the capsule ends.

The resultant phases were identified by XRD using $Cu_{K\alpha}$ radiation (Rigaku RINT 2500). Electron diffraction data were collected between 120 K and room temperature using a JEOL JEM-2010. apparatus. SXRD data were collected at room temperature and 90 K with a large Debye–Scherrer camera installed at BL02B2 (SPring-8).[17] The wavelengths were 0.77699321 and 0.77739787 Å for each run, respectively. The crystal structure was refined with the Rietveld program RIETAN-2000.[18] Magnetic measurements were performed using a SQUID Quantum Design MPMS-XL magnetometer. Electrical resistivity was measured by the standard four-probe method using a Quantum Design PPMS. The ^{57}Fe Mössbauer spectroscopy measurements were performed using a ^{57}Co/Rh γ-ray source at certain fixed temperatures between 4.2 K and room temperature. The velocity scale and the IS were determined relative to α-Fe as reference material, and the resulting spectra were least-squares-fitted using the Lorentzian function.

Received: March 28, 2008
Published online: July 30, 2008

Keywords: charge disproportionation · high-pressure chemistry · magnetic properties · Mössbauer spectroscopy · perovskite phases

[1] P. K. Gallagher, D. N. Buchanan, J. B. MacChesney, *J. Chem. Phys.* **1964**, *41*, 2429.
[2] F. Kanamaru, H. Miyamoto, Y. Mimura, M. Koizumi, M. Shimada, S. Kume, S. Shin, *Mater. Res. Bull.* **1970**, *5*, 257.
[3] Y. Takeda, S. Naka, M. Takano, T. Shinjo, T. Takada, M. Shimada, *Mater. Res. Bull.* **1978**, *13*, 61.
[4] L. Delaude, P. Laszlo, *J. Org. Chem.* **1996**, *61*, 6360.
[5] M. Takano, N. Nakanishi, Y. Takeda, S. Naka, T. Takada, *Mater. Res. Bull.* **1977**, *12*, 923.
[6] P. M. Woodward, D. E. Cox, E. Moshopoulou, A. W. Sleight, S. Morimoto, *Phys. Rev. B* **2000**, *62*, 844.
[7] T. Takeda, R. Kanno, Y. Kawamoto, M. Takano, S. Kawasaki, T. Kamiyama, F. Izumi, *Solid State Sci.* **2000**, *2*, 673.
[8] I. D. Brown, D. Altermatt, *Acta Crystallogr. Sect. B* **1985**, *41*, 244.
[9] The bond valence sum, V_i, is given by $\Sigma_j s_{ij}$ (where $s_{ij} = \exp[(r_0 - r_{ij})/b]$) and was calculated using values of $b = 0.37$ and $r_{ij} =$ 1.679 and 1.772 (as adopted in ref. [6]) for Cu–O and Fe–O, respectively.
[10] J. Sánchez-Benítez, J. A. Alonso, M. J. Martínez-Lope, M. T. Casais, J. L. Martínez, A. de Andrés, M. T. Fernández-Díaz, *Chem. Mater.* **2003**, *15*, 2193.
[11] S. Kawasaki, M. Takano, Y. Takeda, *J. Solid State Chem.* **1996**, *121*, 174.
[12] I. A. Presniakov et al., *Phys. Rev. B* **2007**, *76*, 214407.
[13] H. Falcón, J. Sánchez-Benítez, M. J. Martínez-Lope, J. A. Alonso, K. Krezhov, I. Spirov, T. Ruskov, *J. Phys. Condens. Matter* **2007**, *19*, 356209.
[14] S. Kawasaki, M. Takano, R. Kanno, T. Takeda, A. Fujimori, *J. Phys. Soc. Jpn.* **1998**, *67*, 1529.
[15] M. Mostovoy, *Phys. Rev. Lett.* **2005**, *94*, 137205.
[16] A. E. Bocquet, A. Fujimori, T. Mizokawa, T. Saitoh, H. Namatame, S. Suga, N. Kimizuka, Y. Takeda, M. Takano, *Phys. Rev. B* **1992**, *45*, 1561.
[17] E. Nishibori, M. Takata, K. Kato, M. Sakata, Y. Kubota, S. Aoyagi, Y. Kuroiwa, M. Yamakata, N. Ikeda, *Nucl. Instrum. Methods Phys. Res. Sect. A* **2001**, *467–468*, 1045.
[18] F. Izumi, T. Ikeda, *Mater. Sci. Forum* **2000**, *321–324*, 198.

